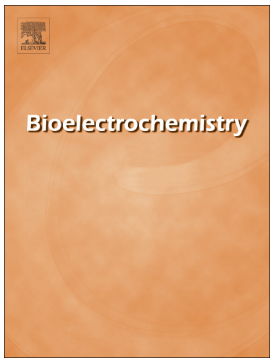

An electrochemical sensing approach for scouting microbial chemolithotrophic metabolism

Albert Saavedra, Federico Figueredo, Eduardo Cortón, Ximena C. Abrevaya

PII: S1567-5394(18)30029-X
DOI: doi:10.1016/j.bioelechem.2018.04.020
Reference: BIOJEC 7156

To appear in: *Bioelectrochemistry*

Received date: 7 February 2018
Revised date: 25 April 2018
Accepted date: 29 April 2018

Please cite this article as: Albert Saavedra, Federico Figueredo, Eduardo Cortón, Ximena C. Abrevaya , An electrochemical sensing approach for scouting microbial chemolithotrophic metabolism. The address for the corresponding author was captured as affiliation for all authors. Please check if appropriate. Biojec(2017), doi:10.1016/j.bioelechem.2018.04.020

An electrochemical sensing approach for scouting microbial chemolithotrophic metabolism

Albert Saavedra[1], Federico Figueredo[1], Eduardo Cortón[1], Ximena C. Abrevaya[2,3]

[1]Laboratorio de Biosensores y Bioanálisis (LABB), Departamento de Química Biológica and IQUIBICEN-CONICET, Facultad de Ciencias Exactas y Naturales. Universidad de Buenos Aires. Ciudad Autónoma de Buenos Aires, Argentina.

[2]Instituto de Astronomía y Física del Espacio (IAFE), CONICET - Universidad de Buenos Aires.Ciudad Autónoma de Buenos Aires, Argentina.

[3]Facultad de Ciencias Exactas y Naturales, Universidad de Buenos Aires. Ciudad Autónoma deBuenos Aires, Argentina.

Corresponding Author: Ximena C. Abrevaya. Address: Pabellón IAFE, Ciudad Universitaria, CC 67, Suc. 28, 1428. Ciudad Autónoma de Buenos Aires, Argentina. Phone: (+54)-11-4788-1916 ext.: 105. Fax: (+54)-11-4786-8114. E-mail: abrevaya@iafe.uba.ar

Abstract

The present study was aimed to test an electrochemical sensing approach for the detection of an active chemolithotrophic metabolism (and therefore the presence of chemolithotrophic microorganisms) by using the corrosion of pyrite by *Acidithiobacillus ferrooxidans* as a model. Different electrochemical techniques were combined with adhesion studies and scanning electron microscopy (SEM). The experiments were performed in presence or absence of *A. ferrooxidans* and without or with ferrous iron in the culture medium (0 and 0.5 gL^{-1}, respectively). Electrochemical parameters were in agreement with voltammetric studies and SEM showing that it is possible to distinguish between an abiotically-induced corrosion process (AIC) and a microbiologically-induced corrosion process (MIC). The results show that our approach not only allows the detection of chemolithotrophic activity of *A. ferrooxidans* but also can characterize the corrosion process. This may have different kind of applications, from those related to biomining to life searching missions in other planetary bodies.

Keywords: *Acidithiobacillus ferrooxidans***,** microbiologically-induced corrosion, biomining, pyrite mineral, *in-situ* life detection.

1. Introduction

Microorganisms have developed different metabolic strategies, along evolutionary timescales on Earth, to obtain energy from different substrates. Metabolic pathways coevolved with environmental physicochemical conditions defining the energy and matter sources available and therefore, the diversity at metabolic level. This includes extreme environments with low availability of organic carbon to sustain metabolisms [1]. An example of a metabolism, present in prokaryotes both from the Bacteria and the Archaea domains that evolved together with some of these environments is the chemolithotrophic one. This type of metabolism is based on the oxidation of inorganic compounds such as hydrogen, ammonia, nitrite, sulfide, elemental sulfur, hydrogen and iron and use carbon dioxide as carbon source.

Particularly, iron is the most abundant element (by weight) that can be found on Earth and the second most abundant metal [2]. Iron can be found in natural environments as part of minerals, as oxides (goethite, magnetite, hematite) and sulfides (pyrite, chalcopyrite, arsenopyrite), and in acidic environments (pH < 2), in soluble form by natural or artificial leaching processes (acid mine drainage). Additionally, iron is also present in high proportions in other planets as Mars. Some of the previously mentioned pyrite minerals as hematite and pyrite were also identified in the Martian soil [3].

Taking advantage of the high amounts of iron on Earth, acidophilic chemolithoautotrophs as *Acidithiobacillus ferrooxidans,* use the oxidation of ferrous iron to obtain energy and in some cases also sulfur ore [4-6]. In terms of its oxygen requirements, *A. ferrooxidans* has been described as an aerobic microorganism even though some studies reported reduction of iron in anaerobic conditions [7,8].

The Tinto River (Huelva, southwestern Spain) that is part of the Iberian Pyritic Belt, is one of the typical acidic environments where chemolitotrophic microorganisms as *A. ferrooxidans* can be found. Due to its characteristics, the Tinto River is also considered a Martian analog. These environments are characterized by corrosion processes that arise when minerals interact with corrosive agents as oxygen and ferric iron in acidic conditions.

Several studies have shown that sulfide minerals as pyrite (FeS_2) can undergo chemical corrosion in aqueous solutions by exposure to dissolved oxygen, where pyrite is oxidized and ferrous iron is released (Eq. 1). Dissolved oxygen can also oxidize ferrous iron to produce ferric iron (E q. 2) that can also oxidize pyrite releasing more ferrous iron (Eq. 4) [9]. Then, a propagation cycle is generated [10].

$$FeS_2 + 3.5O_2 + H_2O \rightarrow Fe^{2+} + 2SO_4^{2-} + 2H^+ \quad (1)$$

$$Fe^{2+} + 0.25\ O_2 + H^+ \rightarrow Fe^{3+} + 0.5H_2O \quad (2)$$

$$Fe^{2+} \xrightarrow{Microorganisms} Fe^{3+} + 1\ e^- \quad (3)$$

$$FeS_2 + 14Fe^{3+} + 8H_2O \rightarrow 15Fe^{2+} + 2SO_4^{2-} + 16H^+ \quad (4)$$

Corrosion and electrochemical oxidation of pyrite by *A. ferrooxidans* was previously identified [11]. Formerly, other authors demonstrated that iron oxidizing

microorganisms can act as catalyzers increasing the iron oxidation rate shown in Eq. (3), and as consequence the corrosion rate [10,12]. Therefore, mineral corrosion can also be induced by microorganisms as *A. ferrooxidans*. This corrosion process is widely known as microbiologically-induced corrosion (MIC) [13]. On the contrary, when ferrous iron is oxidized only by oxygen it is possible to define an abiotically induced corrosion (AIC). In general, in presence of microorganisms both MIC and AIC are contributing to the mineral corrosion process, and in absence of microorganisms only AIC is contributing to the mineral corrosion process.

Moreover, it was shown that some of these acidophilic chemolithoautotrophs are capable to form biofilms on sulfide minerals as pyrite (FeS_2), chalcopyrite ($CuFeS_2$), galena (PbS), and sphalerite (ZnS), among others. Two different mechanisms have been described to coexist in the interaction between acidophilic chemolithoautotrophs and metal sulfide minerals as pyrite [6]: i) An indirect mechanism, where the cells oxidize soluble ferrous iron to ferric iron, which chemically degrades pyrite [14]. ii) A mechanism by contact, where the microorganisms are attached to the surface of the mineral and they start to produce extracellular polymeric substances (EPS) to form a biofilm. These EPS create a microenvironment where iron is accumulated in high concentrations (e.g., more than 53 g L^{-1} of iron in the EPS) [15], therefore the attack acquires a localized form on the surface of the mineral that are seen as etch pits, commonly known as pitting.

Corrosion processes involve both chemical and electrochemical phenomena and sulfide minerals, as pyrite, that are conductors or semiconductors and can be studied by using electrochemical techniques [16,17]. Therefore, an electrochemical sensing of mineral corrosion can be performed using these techniques, having advantages over kinetic methods as they allow a better understanding of the mechanisms behind the process of mineral dissolution [18].

Several electrochemical approaches have been employed to analyze MIC including, among others, cyclic voltammetry and electrochemical impedance spectroscopy. Particularly, chemolithotrophs as *Acidithiobacillus ferrooxidans* and *Leptospirillum ferrooxidans* have been studied in the biocorrosion of stainless steel and minerals found in nature. These studies have shown that several factors can influence the corrosion process, as pH (evaluated from 1.0 to 4.0) and ferric iron concentrations (evaluated from 1.0 a 12.5 g L^{-1}), and have shown that the microorganisms in the presence of ferric iron and a low pH can increase the corrosion process [17].

The goal of this paper is to demonstrate that it is possible not only to measure, but to distinguish an abiotically-induced corrosion (AIC) process from a microbiologically-induced corrosion (MIC) process and therefore, to detect the presence or absence of a chemolithoautotrophic metabolism in a sample. Moreover, previous studies only analyzed the MIC processes in the presence of ferrous iron. In this work we performed experiments both in the presence and absence of ferrous iron to analyze how this can influence both AIC and MIC.

We employed an integrated approach using electrochemical sensing for the detection and identification of the corrosion process based on several electrochemical techniques. As a complementary analysis, cell adhesion studies and scanning electron microscopy were also performed. We used the strict acidophilic chemolithoautotrophic bacteria *A.*

ferrooxidans as model. This microorganism has been extensively studied in different contexts, classically as part of biomining processes. Interestingly, this microorganism also showed to be capable of grow under Mars-like geochemical conditions and also is commonly present in environmental analogs of Mars as The Tinto River. This has opened a particular and interesting new field of study for this microorganism in astrobiology [19]. The methodology we present in this paper may have different future applications for the detection of chemolithotrophic activity in terrestrial or even extraterrestrial environmental samples.

2. Material and methods

2.1. Microorganisms and culture medium

Acidithiobacillus ferrooxidans (strain DSMZ 11477) was employed for the experiments. Cells were grown under agitation at 150 rpm and 30°C in a modified 9K culture medium with the following composition (g L^{-1}): $NH_4H_2PO_4$, 3.0; $MgSO_4 \cdot 7H_2O$, 0.15; KCl, 0.15 and $FeSO_4 \cdot 7H_2O$, 44.0, and adjusted to pH 1.8 [20].

To study the influence of Fe^{2+} in the corrosion of pyrite and therefore in the detection of chemolithotrophic metabolism, the experiments were performed in a medium containing different Fe^{2+} concentrations (of the previously described 9K culture medium) containing 0.5 gL^{-1} of Fe^{2+} (0.5K medium) or without Fe^{2+} (0K medium).

2.2. Corrosion cell architecture and electrodes

Pyrite was obtained from Navajun (Spain). Mineral identity and composition were then verified by X-ray diffraction patterns (XRD Rigaku 22002, Θ=0.02, 10 to 90°, using Cu-Kα radiation) and scanning electron microscopy (SEM, Philips XL30) coupled with an energy dispersive Si(Li) detector (EDAX DX4). Previous to XRD analysis, the samples were pulverized in an agate mortar. This analysis has shown that pyrite (FeS_2) had a purity of 61.82% and additionally contained nacrite ($Al_2Si_2O_5(OH)_4$) (38.18%) (silicate) as impurity. Nacrite does not have electrochemical activity.

Eighteen pyrite electrodes were assembled and used as working electrodes (WE) and were built from the same pyrite crystal to assure a chemical and mineralogical homogeneous composition. Massive pyrite was bound to a brass screw using conductive silver epoxy and subsequently included in epoxy resin (Dystaltec EP System, Buenos Aires, Argentina) in proportions 100:30 resin (DisCat 750) and hardener (DICURE 360) using a 5 mL syringe as a cast. Curing was carried out at 80°C in an oven for 48 h. After removal from the cast, the pyrite side was polished using papers of different grain followed by alumina (up to 0.3 microns), until it acquired a mirror-like appearance. No bubbles or cracks were observed in the WE around the pyrite under a stereomicroscope (Fig.1).

Here Fig.1

Given that natural pyrite mineral pieces were used to make the electrodes; they were not identical. Thus, prior to the experiments, we proceeded to normalize the values of the electrochemical area, by using the cyclic voltammetry (CV) technique, with a scan rate of 25 mV s^{-1} and using as electrolyte 0K medium without shaking (pH=1.8). Then, the

voltammetric charge (Q), definided by $\int_{E_1}^{E_2} I\,(E)dE$, was obtained by integration of positive sweep in cyclic voltammograms. By using the equation reported by Hanlu et al. the overall capacitance (C) was calculated [21]. This was obtained for each electrode (Eq. 5) [21].

$$C=\frac{1/(E_2-E_1)\int_{E_1}^{E_2} I(E)dE}{v} \quad (5)$$

Here, I (A) is the instantaneous current in cyclic voltammograms, v (V s^{-1}) is the scanning rate and E_1, E_2 are the switching potentials in CV [21]. Then, a normalization factor value was obtained by considering the lowest C value obtained with respect to the rest of the electrodes. This normalization value was multiplied by the corrosion current and then the corrosion current density (j_{corr}) was obtained.

Reference electrodes (RE) of Ag/AgCl/KCl_{sat} were made using a previously chlorinated 3 mm diameter Ag wire that was inserted in a micropipette tip (1 mL). The tip was filled with a KCl saturated solution, and the wide end closed with Parafilm (Bemis, Inc.) to minimize the evaporation of the solution. A porous plug was used to minimize leakage. A Luggin capillary was used to improve the quality of our data, by diminishing the effect of ohmic loss. The glass capillary was heat molded with a "J" shape, filled with 2% agar (3 M in KCl); the "J" part was in close contact with the WE (about 1 mm), and the other side in contact with the RE. All potentials obtained in this work were referred to this RE. The stability and potential of the reference electrodes Ag/AgCl/KCl_{sat} (0.199 V vs NHE) were calibrated by using a standard commercial saturated calomel electrode (SCE) (0.24 V vs NHE) (Hanna Instruments, USA) before use. For the calibration we compared the SCE with the reference electrodes Ag/AgCl/KCl_{sat}. The difference between them was of 0.04 V. A graphite bar (Alfa Aesar, 99.999% purity) was used as a counter-electrode (CE).

The corrosion cells were made by using polypropylene flasks (100 mL), filled with 50 mL of culture medium, with a composition according to each the experiment. Four holes were bored in the lids, three of them used to insert the electrodes (WE, RE, and CE), and the last for sample removal.

2.3. Experimental groups

Three different experimental groups were considered: i) *A. ferrooxidans* culture (*ca*. 10^6 cell mL^{-1}), ii) *A. ferrooxidans* sterilized culture (containing dead cells, cellular debris and organic molecules, as a control of some possible effects on the electrodes of those substances) and iii) Culture medium (sterilized culture medium devoid of cells, as an abiotic control).

The first two groups were obtained by using 5 mL of *A. ferrooxidans* culture at exponential phase (*ca*. 10^7 cell mL^{-1}) that was centrifuged (10,000 rpm, 1 min) and resuspended in 5 mL of 0K medium (the procedure was repeated 3 times), in order to eliminate ferric iron and other substances. Then, it was resuspended in 45 mL of 0.5K or 0K medium (according to the experiment). Sterilized cultures obtained following the same procedure but using a sterilized culture of *A. ferrooxidans* (20 min, 125°C). Sterilized culture medium was 0K or 0.5K medium (according to the experiment). The

final working volume for all experiments was 50 mL. The experiments were done in triplicate.

2.4. Bacterial adhesion quantification

The adhesion of *A. ferrooxidans* to the pyrite electrodes was quantified as this step represents the first stage of the biofilm formation [22]. The quantification of the attached cells was performed according to previous studies [22-24]. To this end, 45 mL culture medium (0K or 0.5K) were placed inside the corrosion cells containing the pyrite electrodes. After 24 h, once electrochemical equilibrium was reached, 5 mL of *A. ferrooxidans* culture (*ca*. 10^7 cell mL^{-1}) was inoculated inside the corrosion cells [25]. The experiments were performed inside a shaker at 30°C and 100 rpm. Following 1h of incubation, bacterial adhesion was quantified by taking aliquots of 100 µL and counting planktonic cells of *A. ferrooxidans* using a Neubauer chamber. The amount of bacterial cells that were attached to the mineral was obtained by considering the initial number of cells minus the number of planktonic cells.

2.5. Cell growth quantification and pH measurements

Cell growth was quantified in *A. ferrooxidans* cultures along the experiments. The quantification was done by taking small aliquots (100 µL) of the culture in the corrosion cells. Cell counting was done in a Neubauer chamber.

The pH was not regulated during the experiments and it was monitored for all the experimental groups along time. The initial measured pH value was 1.8.

2.6. Electrochemical analyses of corrosion activity

Different electrochemical techniques were used in order to study corrosion parameters and used to evaluate the possibility to distinguish an abiotically-induced corrosion (AIC) process from a microbiological-induced corrosion (MIC) for *A. ferrooxidans* cultures, sterilized cultures or culture medium that were placed inside the corrosion cells. The measurements were performed along the experiment during 42 days, at 30°C and 100 rpm, both for experiments in 0K and 0.5K medium. The initial measured pH value was 1.8 and it was not regulated during the experiments.

The oxidation-reduction potential (ORP) was used to study the oxidation state of the system being influenced by the concentration of oxidizing and reducing compounds, pH and temperature [26]. The ORP was measured using a commercial ORP electrode (Oakton™ Instruments, IL, USA).

Linear sweep voltammetry (LSV) and open circuit potential (OCP) were the techniques chosen to evaluate AIC and MIC processes on pyrite. The measurements were done using a potentiostat TEQ-03 (Ing. Sobral, La Plata, Argentina) or a Gamry-300 (Gamry Instruments, PA, USA). To choose the potential window for LSV experiments, the OCP was measured for each pyrite electrode at the beginning of each measurement. LSV experiments extended 250 mV to the anodic and cathodic direction from the determined OCP [27]. LSV scan speed was 0.4 mV s^{-1}.

To estimate the evolution AIC and MIC processes on pyrite electrodes, several corrosion parameters, as corrosion potential (E_{corr}), corrosion current density (j_{corr}), and polarization resistance (R_p) were obtained from polarization curves (Log *j* vs. E). The intersection of two tangent lines (Tafel slopes) both for cathodic and anodic sides, in a

potential window of ± 100 mV from the equilibrium potential (E^0), are equivalent to j_{corr} y E_{corr} [28]. The polarization resistance was obtained from the following equation (Eq. 6):

$$R_p = \frac{b_a b_c}{2.3 . j_{corr}(b_a + b_c)} \quad (6)$$

Where R_p is the polarization resistance, b_a and b_c are the cathodic and anodic slopes and j_{corr} is the corrosion current density [27, 29-30].

For comparative purposes, the corrosion rate was calculated for each system, applying the Faraday equation [31]. The displacements in j_{corr} and E_{corr} represents the kinetic behavior of MIC and AIC of pyrite. To estimate the differences in j_{corr} along the experiments and between experimental groups, we considered the j_{corr} rate according to Eq. (7):

$$j_{corr}rate = \frac{\Delta j_{corr}}{\Delta t} = \frac{(j_{corr})_{final} - (j_{corr})_{initial}}{t_{final} - t_{initial}} \quad (7)$$

Where, $(j_{corr})_{initial}$ y $(j_{corr})_{final}$ are the values for j_{corr} at the beginning and end of the experiment, respectively (mA) and t_{final}, $t_{inicial}$ are the values for time, in days, at the beginning and the end of the experiment. Therefore, this j_{corr} value is the product of a cumulative rate along the experiment.

Cyclic voltammetry (CV) was used to study the possible presence of biofilms on the pyrite electrode, seen as interface changes between the mineral and electrolyte. Several CVs were performed at 25 mV s^{-1}, in a potential window from -600 to 800 mV. This was done at the beginning and at the end of the experiments (days 0 and 42). Data obtained were processed applying the first derivative of the CVs. The coefficient of voltammetric charge (Q_c) was determined from the initial and final voltammetric charge (Q_f/Q_i).

2.7. Statistical analysis

A two-way ANOVA with a Tukey test ($F<0.05$) was performed to quantify the differences in the comparison of means values between the experiments or the experimental groups.

2.8. Scanning Electron Microscopy

Once the experiments finished, the electrodes were dismounted and placed in a desiccation chamber. The electrodes were analyzed using a Scanning Electron Microscope (SEM) (Carl Zeiss SUPRA 40). The electrodes were analyzed with a magnification of 10,000X. The samples were not metalized to analyze the possible presence of pitting as a product of corrosion activity on the mineral by *A. ferrooxidans*.

3. Results and discussion

***3.1** Bacterial attachment quantification*

At the beginning of the experiments the influence of ferrous iron on *A. ferrooxidans* attachment to the pyrite electrodes was characterized for *A. ferrooxidans* culture (condition i). The results have shown attachment values of 11.2% (equivalent to 1.18 x 10^6 ± 1.01 x 10^5 cells mL^{-1}) and 31.2% (equivalent to 3.16 x 10^6 ± 5.12 x 10^5 cells mL^{-1})

for experiments performed in 0K and 0.5K medium, respectively (Fig. 2). Therefore, our results support the idea that the presence of ferrous iron in the culture medium may increase the attachment of *A. ferrooxidans* to pyrite.

Bacterial attachment has shown to be the first step related to the biofilm formation [32]. There are several factors that can influence the attachment of microorganisms to the mineral, mainly related to physicochemical and biological phenomena between the bacteria and the mineral. Among these phenomena are attraction by charge [33], chemotaxis [34] and other mechanisms induced by proteins of the bacterial cell membrane that interact directly with the mineral [35].

Our results are in agreement with previous studies showing that ferrous iron may increase chemotaxis and therefore, the adhesion of microorganisms to the mineral [34]. These results are relevant given that previous studies have identified that a greater attachment of the bacterial cells may increase the formation of biofilm, increasing the efficiency of the corrosion process in the mineral [36].

Our bacterial attachment values are lower than those reported in previous studies that have shown bacterial attachment of 80-90% [22,32,37]. This may be due to the architecture and geometric area of the electrodes in our experiments that is much bigger than the particles of mineral used in these previous studies (in general with pyrite grain sizes of 50-100 μm). Small particle sizes may help to an augmented interaction between the bacterial cells and the mineral, obtaining, therefore, a higher bacterial attachment.

Here Fig. 2

3.2. Bacterial growth quantification and pH measurements

Bacterial growth was quantified for *A. ferrooxidans* cultures both for experiments in 0K and 0.5K medium for *A. ferrooxidans* culture (condition i).Bacterial counts of planktonic cells performed along the experiments showed no significant changes along time both for 0K medium ($8.78 \times 10^6 \pm 5.01 \times 10^5$ cells mL^{-1}) and 0.5K medium ($6.56 \times 10^6 \pm 3.12 \times 10^5$ cells mL^{-1}). This could be due to the low duplication rate of *A. ferrooxidans* in comparison with other bacteria and to the culture medium conditions (absence or very low concentration of ferrous iron) [38]. The pH values were measured for all experimental groups and showed an increase from 1.8 ± 0.1 to 2.2 ± 0.3 both for experiments in 0K and 0.5K medium.

Therefore, as bacterial population did not show any significant increase along the experiment both for 0K and 0.5K medium, our results were not influenced by an increase in the number of microorganisms.

3.3. Electrochemical analyses of corrosion activity

In order to study the oxidation state of the system for all the experimental groups, the ORP values were measured over time both for the experiments performed in 0K and 0.5K medium.

The results have shown very slight variations of ORP values over time for all experimental groups in experiments performed in 0K medium, *A. ferrooxidans* culture shown an ORP along time from 312 ± 16.1 mV. For sterilized culture and culture medium the ORP was from 319 ± 21.3 and 315 ± 14.4 mV, respectively (Fig.S1B,

supplementary material). In contrast, the ORP values in experiments performed in 0.5K medium, have shown variations over time. Particularly, *A. ferrooxidans* culture has shown an increase in the ORP along time from 402 ± 9.2 to 576 ± 15.1 mV. For sterilized culture and culture medium the increase in the ORP was from 404±21.8 to 481 ± 7.53 mV and from 416 ± 4.8 to 467 ± 12.1 mV, respectively (Fig. S1 B, supplementary material). The differences obtained for both experiments may be explained by the presence or absence of ferrous iron in aqueous solution for 0.5K and 0K medium, respectively.

Previous studies using massive pyrite in culture medium with very low iron concentrations (0.01 g mL^{-1} $FeSO_4.7H_2O$), have shown the formation of non-stoichiometric compounds of low conductivity ($Fe_{1-x}S_{2(x)}$) at potentials near the open circuit potential, given by the Eq. (8) [39]:

$$FeS_{2(x)} \leftrightarrow Fe_{1-x}S_{2(x)} + xFe^{2+}_{(l)} + (2x)e^{-} \quad (8)$$

These compounds may be also present in our experiments when 0K medium is employed, therefore explaining the low ORP values obtained in these conditions. Additionally, other studies documented similar ORP values in absence of ferrous [40].

The ORP values obtained for our experiments 0.5K medium may be related to the presence of ferric iron in aqueous solution. Moreover, the increase in ORP values for *A. ferrooxidans* cultures in 0.5K medium, may be due mainly to bacterial oxidation of soluble ferrous iron by *A. ferrooxidans* (Eq. 3) and also by the oxidation of pyrite by abiotic chemical mechanisms that were shown previously in Eq. (1), (2), and (4) (section 1) [41,42]. Additionally, our results related to bacterial attachment (section 3.1) have shown that ferrous iron increases the bacterial attachment to pyrite. This may favor the biofilm formation, thus increasing the oxidation of pyrite.

In contrast, sterilized cultures and culture medium samples in 0.5K medium have shown lower ORP values than those obtained for *A. ferrooxidans* culture, due to the absence of microbial oxidation and only due to abiotic mechanisms [42,43].

The corrosion activity on the pyrite electrodes was analyzed through polarization curves (Fig. 3). The corrosion density current (j_{corr}), polarization resistance (R_p) and corrosion potential (E_{corr}) values were obtained and a comparison was done for the values at the beginning and at the end of the experiments performed in 0K and 0.5K medium (Table 1).

The comparison between polarization curves at the beginning and at the end of the experiments, for *A. ferrooxidans* cultures in 0K medium, have shown an increase in j_{corr} and a decrease in R_p (Fig. 3 A). The j_{corr} values for the same group have shown an increase from (mean ± SD) 0.59 ± 0.11 to 6.02 ± 2.03 µA and the R_p values have shown a decrease from 330.64 ± 98.12 to 41.75 ± 11.19 Ω. These results may be explained by the presence of an active microbiologically-induced corrosion (MIC) process.

On the contrary, j_{corr} y R_p values for sterilized cultures and culture medium were similar throughout the experiments (Fig. 3 B, C). The j_{corr} values for both sterilized cultures and culture medium have shown a very slight increase from (mean ± SD) 0.67 ± 0.06 to 0.91 ± 0.04 µA, and 1.01 ± 0.09 to 1.10 ± 0.01 µA respectively. The R_p values for the

same experimental groups have shown a slight decrease of (mean ± SD) 158.38 ± 36.33 to 224.09 ± 51.02 Ω, and 219.36 ± 98.12 to 216.01 ± 74.31 Ω, respectively (Table 1). These results may be explained by an inactive corrosion process in the absence of microorganisms.

Moreover, the comparison between both groups for j_{corr} values have shown significant differences between *A. ferrooxidans* cultures and sterilized cultures and culture medium (F<0.05). The comparison between *A. ferrooxidans* cultures and culture medium have shown non-significant differences (F>0.05). The same comparison for R_p values have shown significant differences between all groups (F<0.05). The E_{corr} values for experiments in 0K medium have shown a positive displacement for all groups (Fig. 3 A, B, C) (Table 1). No significant differences were observed in the comparison between experimental groups (F>0.05).

The comparison between polarization curves at the beginning and at the end of the experiments for *A. ferrooxidans* cultures in 0.5K medium, have shown a high increase in j_{corr} and a high decrease in R_p (Fig. 3 A). The j_{corr} values for *A. ferrooxidans* cultures have shown an increase from (mean ± SD) 0.64 ± 0.09 to 24.51 ± 4.73 µA and the R_p values have shown a decrease from (mean ± SD) 197.58 ± 51.17 to 7.17 ± 4.25 Ω.

These results may be explained by an increase in the Eq. (3) (section 1), given both by the presence of microorganisms (increasing a MIC related process) and by the presence of ferrous iron in the culture medium (increasing an AIC related process) that is oxidized to ferric iron by oxygen. This may also explain why these values are higher than those obtained for 0K medium experiments where MIC is the main process.

On the contrary, sterilized cultures have shown a slight increase in j_{corr} values from (mean ± SD) 3.28 ± 0.05 to 4.56 ± 2.19 µA and a slight decrease in R_p values from (mean ± SD) 462.82 ± 96.23 to 400.85 ± 101.24 Ω. Meanwhile, culture medium has shown an increase in j_{corr} values from (mean ± SD) 0.93 ± 0.12 to 4.61 ± 2.13 µA and a decrease in R_p values from (mean ± SD) 145.54 ± 31.13 to 60.11 ± 21.11 Ω, that was greater than those obtained for sterilized cultures (Fig. 3 B, C). These results may be related to the absence of MIC and the differences observed between the latter groups to a passivation process in the sterilized cultures, due to the presence of cellular debris [44].

Moreover, the comparison between groups for j_{corr} values have shown significant differences between *A. ferrooxidans* culture and sterilized cultures and culture medium (F<0.05). The comparison between *A. ferrooxidans* culture and culture medium have shown non-significant differences (F>0.05). The same comparison for R_p values have shown significant differences between *A. ferrooxidans* cultures and sterilized cultures (F<0.05). However, the comparison between *A. ferrooxidans* cultures and culture medium have shown non-significant differences (F>0.05). The comparison between sterilized culture and culture medium have shown significant differences (F>0.05).

The E_{corr} values for experiments in 0.5K medium in general have shown a positive displacement (Fig. 3 A, B, C) (Table 1). The comparison between groups have shown significant differences between *A. ferrooxidans* cultures and sterilized groups (F<0.05), however the rest of the comparisons have shown non-significant differences (F>0.05).

Our results are in agreement with previous studies that have shown that the displacement of E_{corr} is related to the compositional changes of the medium. For 0K medium, there is a minimum positive displacement for all groups that is due to Eq. (8), described in the manuscript. Here, the oxidizing agent (ferrous iron) solubilized from the mineral, increases the E_{corr} and predispose the pyrite to a corrosive process. For 0.5K medium, this displacement is higher, due to a higher concentration of the oxidizing agent (the ferrous iron solubilized from the mineral plus the ferrous iron present on the medium). Previous studies have characterized these phenomena and they have linearized the response of E_{corr} as function of the concentration of oxidizing agent [45].

Meanwhile the changes in the j_{corr} may be related to an increase of the reactive area and to a deposition of electroactive compounds in the corrosion process, where a decrease in the R_p values is observed [46].

Here Fig. 3

Here Table 1

Thereafter, we studied the j_{corr} rates for different experimental groups in 0K and 0.5K medium (Fig. 4). *A. ferrooxidans* culture, sterilized cultures and culture medium in experiments with 0K medium have shown j_{corr} rates of (mean ± SD) 0.09 ± 0.04, 0.0023 ± 0.0012 and 0.003 ± 0.002, respectively. The comparisons between the mean values of j_{corr} rates of *A. ferrooxidans* cultures and both sterilized cultures and culture medium have shown significant differences ($F<0.05$). These significant differences and the high mean values of j_{corr} rates for *A. ferrooxidans* cultures in comparison with the other groups can be attributed to MIC, due to the presence of an active metabolism of *A. ferrooxidans*, in the aforementioned condition. On the contrary, the comparison between the mean values of j_{corr} rates of sterilized culture and culture medium have shown no significant differences ($F>0.05$). The absence of significant differences between these groups and their low mean values of j_{corr} rates may be attributable to chemical corrosion processes (abiotic) due to the interaction between culture medium and the mineral.

A. ferrooxidans culture, sterilized cultures and culture medium in experiments with 0.5K medium have shown j_{corr} rates of (mean ± SD) 0.54 ± 0.09, 0.012 ± 0.006 and 0.093 ± 0.009, respectively. The comparison between mean values of j_{corr} rates of *A. ferrooxidans* cultures and both sterilized cultures and culture medium have shown significant differences. As was described for the experiments in 0K medium, these significant differences and the high mean values of j_{corr} rates of *A. ferrooxidans* cultures in comparison with the other groups can be attributed to MIC, due to the presence of an active metabolism of *A. ferrooxidans*, in *A. ferrooxidans* culture. The comparison between mean values of j_{corr} rates of sterilized culture and culture medium have also shown significant differences ($F<0.05$). The low mean values of j_{corr} rates obtained for sterilized cultures and the significant differences seen for this comparison are probably due to chemical corrosion induced by ferric iron present in the culture medium and passivation of the pyrite in sterilized cultures. A possible explanation may be attributed to the fact that organic debris of bacteria present in sterilized cultures together with ferric iron may form a film layer and it may be deposited on the surface of the pyrite electrode. Previous experimental studies where the presence of EPS was simulated without the presence of bacteria have shown that EPS on the surface of mineral reduce oxygen transfer and passivate pyrite [44]. In our case we may have a similar effect due

to cellular debris deposited on the surface of the pyrite electrodes.

Additionally, we made a comparison between mean values of j_{corr} rates of *A. ferrooxidans* cultures from experiments performed both in 0 and 0.5K medium conditions. This comparison has shown significant differences ($F<0.05$). The high mean values of j_{corr} rates obtained for 0.5K medium can be attributed to biological oxidation of ferrous iron by MIC, chemical oxidation of ferrous iron and by the chemical catalytic effect of ferric iron, all in combination. The comparison between mean values of j_{corr} rates of sterilized cultures from experiments performed both in 0 and 0.5K medium conditions have shown no significant differences ($F>0.05$). In this case it may be due to the presence of compounds on the surface of the pyrite electrode that can induce passivation, and therefore chemical corrosion prevented, even in the presence of ferric iron in 0.5K medium. The same comparison was done for culture medium that have shown significant differences ($F<0.05$). These differences are attributable to chemical corrosion in the presence or absence of ferric and ferrous iron.

It was possible to estimate the difference between AIC and MIC from the j_{corr} rate values obtained for *A. ferrooxidans*culture (MIC + AIC) and j_{corr} rate obtained for culture medium (AIC). For 0K medium there is a relation MIC:AIC of 30:1. For 0.5K the relation was 5.48:1. This relation is lower for 0.5K medium, given that the Eq. (4) is increased by the contribution of ferric iron coming from the ferrous iron in the medium (Fig. 4, insert).

Here Fig. 4

The electrochemical corrosion rate of pyrite was also calculated from Faraday's equation. Moreover, the Faraday equation was previously employed in different studies to evaluate, under the electrochemical point of view, the corrosion rate of different mineral electrodes [31,47,48]. This computes the kinetics of the cathodic and anodic reactions or the oxidation-reduction. The results have shown, both for 0K and 0.5K medium, that the rates are very different between *A. ferrooxidans* cultures, sterilized cultures and culture medium (Fig. 5).

Our results for experiments in 0K medium have shown that for *A. ferrooxidans* culture, the increase in the corrosion rate is continuous (Fig 5A) meanwhile for sterilized culture and culture medium there is no increase in the corrosion rate (Fig. 5B and 5C, respectively). For *A. ferrooxidans* cultures the highest corrosion rate mean value was $(4.89 \pm 2.01).10^{-7}$ mol. s^{-1}, and for sterilized cultures and culture medium the mean values were $(6.98 \pm 3.1).10^{-8}$ mol. s^{-1}, $(1.32 \pm 0.24).10^{-7}$ mol. s^{-1}, respectively. The increase in the corrosion rate values is due to MIC of *A. ferrooxidans*, as was shown in other systems [49,50]. In this case, as ferrous iron is not present in the culture medium, ferrous iron can be available to the bacterium on the surface of pyrite through the interaction between the pyrite electrode and the culture medium, as was described by the Eq. (8) and then, ferrous iron can be oxidized by the bacterium by the Eq. (3). The increase in the corrosion rates may be due to the existence of an iron oxidation-reduction propagation cycle between Eq. (8) and (3), that leads to the accumulation of ferric iron over time.

Our results for 0.5K medium have shown that for *A. ferrooxidans* culture, the increase in the corrosion rate is continuous (Fig. 5D) meanwhile, for sterilized culture and

culture medium there is no increase in the corrosion rate (Fig. 5E and 5F, respectively). For *A. ferrooxidans*cultures the highest corrosion rate mean value was $(24.7 \pm 8.2).10^{-7}$ mol. s^{-1} and for sterilized cultures and culture medium the mean values were $(4.35 \pm 0.98).10^{-7}$ mol. s^{-1} $(3.26 \pm 1.61).10^{-7}$ mol. s^{-1}, respectively. The very high corrosion rate values obtained for *A. ferrooxidans* cultures are due to MIC of *A. ferrooxidans* described by Eq. (3) but also to AIC processes, as described in the Eq. (1), (2) and (4). Here, there is also an iron oxidation-reduction propagation cycle that is increased by the presence of ferrous iron in the culture medium. In fact, a comparison made between the oxidation rate of ferrous iron under sterile conditions (abiotic conditions) and the oxidation rate of ferrous iron after inoculation with microorganisms as *A. ferrooxidans* have demonstrated that iron oxidizing microorganisms can increase the iron oxidation rate by a factor larger than 10^6 [10,12].

For sterilized culture and culture medium, the increase of the corrosion rate is negligible. In this case, our results may be explained by Eq. (1), (2) and (4). However, given the absence of bacteria in these groups the oxidation of ferrous iron in Eq. (2) is only abiotic and mediated by oxygen, at lower rates, hence limiting Eq. (1) and (4).

Therefore, the j_{corr} values in *A. ferrooxidans* culture are the consequence of the addition of both AIC and MIC processes. To estimate the j_{corr} related only to the MIC process, it is possible to calculate the difference of j_{corr} obtained for *A. ferrooxidans* culture (MIC+AIC) and culture medium (AIC). The difference between this two j_{corr} values corresponds only to j_{corr} of the MIC process. These values were 4.3 ± 1.9 and 15.2 ± 3.2 µA for 0K y 0.5K medium, respectively.

The difference between replicates for *A. ferrooxidans* cultures may be due to the electrode area. Even though the electrode area was normalized in our calculations, the bacterial attack to the mineral is dissimilar for each case, resulting in a different reactive area. This may be related to the pitting over the pyrite electrodes at the end of the experiments, as will be shown in section 3.4.

Moreover, the comparison between of corrosion rates values for *A. ferrooxidans* cultures and sterilized culture have shown significant differences. However, non-significant differences were seen for the comparison between *A. ferrooxidans* culture and culture medium and for sterilized culture and culture medium.

Here Fig. 5

3.4. Cyclic voltammetric study

To study the interface changes in the pyrite electrode, cyclic voltammetries (CVs) for experiments performed in 0K and 0.5K medium were evaluated at the beginning and the end of the experiment and the coefficient of voltammetric charge (Q_c) was estimated (Fig. 6).

For 0K medium experiments, *A. ferrooxidans* cultures have shown a Q_c mean value of 5.48 ± 1.21. Sterilized cultures and culture medium have shown Q_c mean values of 1.46 $\pm$ 0.17 and 1.42 ± 0.43, respectively. The Q_c values for non-sterilized cultures were five times higher than those for sterilized cultures and culture medium. This may be due the formation of electroactive compounds by the catalytic activity of the bacterium on the pyrite electrode surface.

The comparison between the Q_c values for *A. ferrooxidans* cultures and the other groups have shown significant differences (F<0.05). However, the comparison between sterilized culture and culture medium have shown non-significant differences (F>0.05).

For 0.5K medium experiments, *A. ferrooxidans* cultures have shown a Q_c mean value of 8.73 ± 2.31. Sterilized cultures and culture medium have shown a mean value of 1.45 ± 0.25 and 1.42 ± 0.51, respectively. The Q_c values for *A. ferrooxidans* cultures were five times higher than those for sterilized cultures and culture medium. This high Q_c values may be explained by the same mechanisms for 0K medium but also by other additional mechanisms that coexist due to the presence of ferrous iron in the culture medium, that may alter the interface of the pyrite electrode. Previous studies using *A. ferrooxidans* have also shown similar results [51].

The comparison between the Q_c values for *A. ferrooxidans* cultures and the other groups have shown significant differences (F<0.05). However, the comparison between sterilized culture and culture medium have shown non-significant differences (F>0.05).

In general, all these results are well correlated with those obtained by the corrosion rates obtained previously. The changes in the Q_c values are related to changes in the electrode area by the formation of electroactive and/or passive compounds [52].

Additionally, the presence of faradaic current peaks was analyzed in CVs. For 0K medium experiments, faradaic current peaks were not observed (Fig. 6 A, B, C). Nevertheless, when applying the first derivative of the CVs, an anodic current peak at +458mV were observed for *A. ferrooxidans* cultures (Fig.S2 supplementary material).

For 0.5K medium, several current peaks were observed for sterilized culture and culture medium (Fig. 6 D, E, F). *A. ferrooxidans* cultures have shown a current peak when applying the first derivative, resulting in an increase of the anodic current peak at +458mV with respect to 0K medium. Several additional anodic peaks were also identified at -261,-185, -88 and +17 mV and cathodic peaks at +458, +17, -217 and -488mV (Fig. S2). These current peaks are related to the oxidation and reduction during the dissolution of pyrite [39].

Interestingly, the coincidence of anodic and cathodic current peaks at +458 and +17 mV indicates the presence of adsorbed compounds over the pyrite electrode. This may be due to the presence of biofilms or the electroactive compounds on the surface of the mineral. Previous studies have described the presence of a complex between membrane proteins of *A. ferrooxidans* (rusticyanin and cytochrome c4) and the electrode. These faradaic current peaks are described with potentials of +350 mV (reduction) and +460 mV (oxidation) [53-55]. Carbajosa et al., describes a peak at 45 mV that may be related with the metabolic capabilities of the microorganisms, specifically of the cytochrome c that is associated with iron oxidation [53]. The current peaks obtained in our experiments are very similar to those obtained in previous studies and may be, therefore, the evidence of the interaction between the bacteria and the pyrite.

Sterilized cultures have shown an irreversible current peak identified at +450 mV (peak c) (Figure 6E). This may be related to the formation of compounds as iron hydroxide complexes, [56] that can induce passivation as shown in Eq. (11).

Culture medium have shown four anodic current irreversible peaks, at 70 mV (peak a), Eq. (9), 165 mV (peak b), Eq. (10) and 450 mV (peak c), Eq. (11) and a cathodic peak at -108 mV (peak d) (Figure 6F). These current peaks were previously reported by other authors and may be related to pyrite oxidation [57] Eq. (12).

$$S^0 + 2H^+ + 2e^- \rightarrow H_2S \quad (9)$$

$$FeS_2 \rightarrow Fe^{2+} + 2S^0 + 2e^- \quad (10)$$

$$Fe^{2+} + 3H_2O \rightarrow Fe(OH)_3 + 3H^+ + e^- \quad (11)$$

$$FeS_2 + 2H^+ + 2e^- \rightarrow FeS + H_2S \quad (12)$$

The presence of these irreversible current peaks, corresponding to different chemical reactions suggests that in abiotic processes, iron hydroxides and S^0 are formed on the surface of the pyrite electrode.

Here Fig. 6

3.5. Scanning Electron Microscopy (SEM)

As bacterial adhesion quantification showed an increased attachment of the cells to the surface of the pyrite electrode for 0.5K medium (section 3.1), a mechanism of corrosion may be favored in this medium. Therefore, to confirm these observations, we analyzed bacterial attachment to the pyrite electrodes through SEM after the completion of the experiments. SEM images of the surface of pyrite electrodes were taken before and after the experiments in 0.5K medium for *A. ferrooxidans* culture, sterilized culture and culture medium (10, 000X).

SEM studies of the surface of the pyrite electrodes before the beginning of the experiments areshown in Fig. 7. The structure of the mineral can be seen in the absence of corrosion (Fig. 7A). The mineral surface of the electrode after the experiments in *A. ferrooxidans* cultures is shown in Fig. 7B. Signals of weathering as product of corrosion activity can be seen in the form of extremely localized corrosion areas as etch pits or pitting. This may be explained by the corrosion induced by *A. ferrooxidans* where a contact mechanism is involved through the presence of EPS produced by the bacterium biofilm on the pyrite surface. It is supposed that the EPS creates a microenvironment where the concentration of iron and sulfur are increased, therefore producing these localized areas of corrosion. A scheme of this mechanism is shown in Fig. 8. Several studies support the idea that *A. ferrooxidans* cells could be attached to the surface of the mineral and form pitting [58,59]. Fig.8B shows a magnification of this pyrite electrode where the etch pits of the bacteria can be seen deduced from their size (*A. ferrooxidans* is a bacillus with a size around 1.5 x 0.5 µm). This is in agreement with the results of the electrochemical experiments that have shown an increase in the reactive area of the electrode as was observed by the increase in j_{corr} and the decrease in R_p and then also corroborated by the voltammetric studies (Section 3.3 and 3.4)

In comparison, the surface of the mineral exposed both to sterilized culture (Figure 7C) and culture medium (Figure 7D) shows a slight corrosion with some crystals as product of chemical corrosion processes. Previous works have shown that compounds other than

jarosite and elemental sulfur, as ferric phosphate ($FePO_{4(s)}$) may precipitate on the surface of pyrite when ferric iron is present in culture medium [39].

Here Fig. 7

Here Fig. 8

4. Conclusions

In this study we demonstrated that the electrochemical approach employed may distinguish a microbiologically-induced corrosion (MIC) process from an abiotically-induced corrosion (AIC) process.

However, the presence of ferrous iron in the culture medium influences both AIC and MIC and the corrosion effects are enhanced when iron is present.

Bacterial growth did not show any increase along the experiment both for 0K and 0.5K medium, therefore our results were not influenced by an increase in the number of microorganisms. However, bacterial attachment was favored when iron was present in experiments performed in 0.5K medium.

Moreover, the increase in ORP was observed only when iron was present in the culture medium, and in particular for non-sterilized cultures due to microbial oxidizing activity of *A. ferrooxidans*.

The electrochemical parameters j_{corr} and R_p, have shown to increase and decrease respectively, when MIC process is present. Statistical analysis has shown that it is possible to use them to discriminate an AIC from a MIC. However, for R_p values in 0.5K medium experiments, non-sterilized cultures have shown non-significant differences when compared with culture medium. This means that in this case, AIC process cannot be clearly distinguished form MIC process. Therefore, j_{corr} seems to be a better parameter to unequivocally distinguish both processes.

Even though E_{corr} values can provide some information of the corrosion process, this parameter have shown to be not useful to discriminate AIC from MIC.

When dynamical electrochemical parameters as j_{corr} rate and corrosion rate where evaluated, it was shown that the values are higher when MIC is present.

The voltammograms have shown an increase in the Q_c values, indicating an increase in the electrode area and the presence of an electroactive biofilm. This was evidenced when obtaining the first derivative of the voltammogram and then confirmed by SEM images, showing the presence of edge pitches due to MIC.

Meanwhile in abiotic conditions faradic current peaks where observed, due to the presence of compounds that can induce passivation as elemental sulfur and iron hydroxides. Statistical analysis of the Q_c values has shown that this is also an appropriate electrochemical parameter to discriminate AIC from MIC.

In conclusion, our study provides a set of electrochemical parameters that can be used as an electrochemical approach, not only to detect the sulfur iron oxidizing process

performed by microorganisms but to characterize the corrosion process itself, having additional applications in the evaluation of biomining processes, as the study of mineral corrosion (pyrite or other sulphide minerals) by iron oxidizing microorganisms (e.g.: *Leptospirillum ferrooxidans*, *Leptospirillum ferriphillum*, among others) or sulfur oxidizing microorganisms (Ej. *Acidithiobacillus thiooxidans, Sulfolobus* sp, among others).

Supplementary data

E-supplementary data of this work can be found in online version of the paper.

Authors' contributions:

A.S. performed the experiments, collected, processed and analyzed data, was involved in the study design and contributed to writing of the manuscript. F.F. provided support for the experiments. E.C. provided the facilities, funding, revised and commented on the manuscript. X.C.A. proposed and designed the idea and the study, was involved in data analysis and discussed the results with the authors and was in charge of the organization and writing of the whole manuscript.

Acknowledgements

We want to acknowledge CONICET for A Saavedra PhD scholarship. This work was supported by the University of Buenos Aires (UBA), the National Council for Scientific and Technological Research (CONICET), and the National Agency of Scientific and Technological Promotion (ANPCyT), by the grants "BID-PICT 2013-0033" and "BID-PICT 2014-0402".

We would like to thank the anonymous reviewers that helped to enhance the quality of the manuscript.

References

[1] A.S. Templeton, Geomicrobiology of iron in extreme environments, Elements. 7 (2011) 95–100.

[2] S. Hedrich, M. Schlomann, D.B. Johnson, The iron-oxidizing proteobacteria, Microbiology. 157 (2011) 1551–1564.

[3] M.Y. Zolotov, E.L. Shock, Formation of jarosite-bearing deposits through aqueous oxidation of pyrite at Meridiani Planum, Mars, Geophys. Res. Lett. 32 (2005) L21203.

[4] A.B. Jensen, C. Webb, Ferrous sulphate oxidation using *Thiobacillus ferrooxidans*: a review, Process Biochem. 30 (1995) 225–236.

[5] O.H. Tuovinen, D.P. Kelly, Studies on the growth of *Thiobacillus ferrooxidans*, Arch. Mikrobiol. 88 (1973) 285–298.

[6] M. Vera, A. Schippers, W. Sand, Progress in bioleaching: fundamentals and mechanisms of bacterial metal sulfide oxidation—part A, Appl. Microbiol. Biotechnol. 97 (2013) 7529–7541.

[7] N. Ohmura, K. Sasaki, N. Matsumoto, H. Saiki, Anaerobic respiration using Fe^{3+}, S^0, and H_2 in the chemolithoautotrophic bacterium *Acidithiobacillus ferrooxidans*, J. Bacteriol. 184 (2002) 2081–2087.

[8] H. Osorio, S. Mangold, Y. Denis, I. Nancucheo, M. Esparza, D.B. Johnson, V. Bonnefoy, M. Dopson, D.S. Holmes, Anaerobic sulfur metabolism coupled to dissimilatory iron reduction in the extremophile *Acidithiobacillus ferrooxidans*, Appl. Environ. Microbiol. 79 (2013) 2172–2181.

[9] M. Gleisner, R.B. Herbert, P.C. Frogner Kockum, Pyrite oxidation by *Acidithiobacillus ferrooxidans* at various concentrations of dissolved oxygen, Chem. Geol. 225 (2006) 16–29.
[10] P.C. Singer, W. Stumm, Acidic mine drainage: the rate-determining step, Science 167 (1970) 1121–1123.
[11] C. Pisapia, B. Humbert, M. Chaussidon, C. Mustin, Perforative corrosion of pyrite enhanced by direct attachment of *Acidithiobacillus ferrooxidans*, Geomicrobiol. J. 25 (2008) 261–273
[12] M.P. Silverman, H.L. Ehrlich, Microbial formation and degradation of minerals, in: 1964: pp. 153–206.
[13] N. Kip, J.A. van Veen, The dual role of microbes in corrosion, ISME J. 9 (2015) 542–551.
[14] T.D. Brock, J. Gustafson, Ferric iron reduction by sulfur- and iron-oxidizing bacteria., Appl. Environ. Microbiol. 32 (1976) 567–71.
[15] W. Sand, T. Gehrke, Extracellular polymeric substances mediate bioleaching/biocorrosion via interfacial processes involving iron(III) ions and acidophilic bacteria, Res. Microbiol. 157 (2006) 49–56.
[16] K. Osseo-Asare, Semiconductor electrochemistry and hydrometallurgical dissolution processes, Hydrometallurgy. 29 (1992) 61–90.
[17] H. Tributsch, J.. Rojas-Chapana, Metal sulfide semiconductor electrochemical mechanisms induced by bacterial activity, Electrochim. Acta. 45 (2000) 4705–4716.
[18] G. Debernardi, C. Carlesi, Chemical-electrochemical approaches to the study passivation of chalcopyrite, Miner. Process. Extr. Metall. Rev. 34 (2013) 10–41.
[19] A. Bauermeister, P. Rettberg, H.C. Flemming, Growth of the acidophilic iron–sulfur bacterium *Acidithiobacillus ferrooxidans* under Mars-like geochemical conditions, Planet. Space Sci. 98 (2014) 205–215.
[20] T.W. Kim, C.J. Kim, Y.K. Chang, H.W. Ryu, K.S. Cho, Development of an optimal medium for continuous ferrous iron oxidation by immobilized *Acidothiobacillus ferrooxidans* cells, Biotechnol. Prog. 18 (2002) 752–759.
[21] H. Li, J. Wang, Q. Chu, Z. Wang, F. Zhang, S. Wang, Theoretical and experimental specific capacitance of polyaniline in sulfuric acid, J. Power Sources. 190 (2009) 578–586.
[22] B. Florian, N. Noël, C. Thyssen, I. Felschau, W. Sand, Some quantitative data on bacterial attachment to pyrite, Miner. Eng. 24 (2011) 1132–1138.
[23] R.L. Yu, Y. Ou, J.X. Tan, F.D. Wu, J. Sun, L. Miao, D.L. Zhong, Effect of EPS on adhesion of *Acidithiobacillus ferrooxidans* on chalcopyrite and pyrite mineral surfaces, Trans. Nonferrous Met. Soc. China 21 (2011) 407–412.
[24] J. Liu, Q. Li, W. Sand, R. Zhang, Influence of *Sulfobacillus thermosulfidooxidans* on initial attachment and pyrite leaching by thermoacidophilic archaeon *Acidianus* sp. DSM 29099, Minerals. 6 (2016) 76.
[25] R. Cruz, I. Lázaro, I. González, M. Monroy, Acid dissolution influences bacterial attachment and oxidation of arsenopyrite, Miner. Eng. 18 (2005) 1024–1031.
[26] H. Liu, H. Yin, Y. Dai, Z. Dai, Y. Liu, Q. Li, H. Jiang, X. Liu, The co-culture of *Acidithiobacillus ferrooxidans* and *Acidiphilium acidophilum* enhances the growth, iron oxidation, and CO_2 fixation, Arch. Microbiol. 193 (2011) 857–866.
[27] M. Stern, A.L. Geaby, Electrochemical polarization, J. Electrochem. Soc. 104 (1957) 56.
[28] X.L. Zhang, Z.H. Jiang, Z.P. Yao, Y. Song, Z.D. Wu, Effects of scan rate on the potentiodynamic polarization curve obtained to determine the Tafel slopes and

corrosion current density, Corros. Sci. 51 (2009) 581–587.
[29] R. Bandy, D.A. Jones, Analysis of errors in measuring corrosion rates by linear polarization, Corrosion. 32 (1976) 126–134.
[30] F. Mansfeld, Tafel slopes and corrosion rates obtained in the pre-Tafel region of polarization curves, Corros. Sci. 47 (2005) 3178–3186.
[31] R.M. Luna-Sánchez, I. González, G.T. Lapidus, A Comparative study of silver sulfide oxidation in cyanide media, J. Electrochem. Soc. 150 (2003) D155.
[32] T.R. Garrett, M. Bhakoo, Z. Zhang, Bacterial adhesion and biofilms on surfaces, Prog. Nat. Sci. 18 (2008) 1049–1056.
[33] R.C. Blake, E.A. Shute, G.T. Howard, Solubilization of minerals by bacteria: electrophoretic mobility of *Thiobacillus ferrooxidans* in the presence of iron, pyrite, and sulfur., Appl. Environ. Microbiol. 60 (1994) 3349–57.
[34] G. Meyer, T. Schneider-Merck, S. Böhme, W. Sand, A simple method for investigations on the chemotaxis of *A. ferrooxidans* and *D. vulgaris*, Acta Biotechnol. 22 (2002) 391–399.
[35] A. Klingl, C. Moissl-Eichinger, G. Wanner, J. Zweck, H. Huber, M. Thomm, R. Rachel, Analysis of the surface proteins of *Acidithiobacillus ferrooxidans* strain SP5/1 and the new, pyrite-oxidizing *Acidithiobacillus* isolate HV2/2, and their possible involvement in pyrite oxidation, Arch. Microbiol. 193 (2011) 867–882.
[36] J. Zhu, X. Huang, F. Zhang, L. Feng, J. Li, Inhibition of quorum sensing, biofilm, and spoilage potential in *Shewanella baltica* by green tea polyphenols, J. Microbiol. 53 (2015) 829–836.
[37] K. Harneit, A. Göksel, D. Kock, J.H. Klock, T. Gehrke, W. Sand, Adhesion to metal sulfide surfaces by cells of *Acidithiobacillus ferrooxidans*, *Acidithiobacillus thiooxidans* and *Leptospirillum ferrooxidans*, Hydrometallurgy. 83 (2006) 245–254.
[38] C.J.. Dempers, A.. Breed, G.. Hansford, The kinetics of ferrous-iron oxidation by *Acidithiobacillus ferrooxidans* and *Leptospirillum ferrooxidans*: effect of cell maintenance, Biochem. Eng. J. 16 (2003) 337–346.
[39] R.H. Lara, J. Vazquez-Arenas, G. Ramos-Sanchez, M. Galvan, L. Lartundo-Rojas, Experimental and theoretical analysis accounting for differences of pyrite and chalcopyrite oxidative behaviors for prospective environmental and bioleaching applications, J. Phys. Chem. C. 119 (2015) 18364–18379.
[40] A. Ahmadi, Influence of ferric and ferrous iron on chemical and bacterial leaching of copper flotation concentrates, Int. J. Nonferrous Metall. 1 (2012) 42–48.
[41] D.B. Johnson, T. Kanao, S. Hedrich, Redox transformations of iron at extremely low ph: fundamental and applied aspects, Front. Microbiol. 3 (2012).
[42] A. Saavedra, E. Donati, E. Cortón, Reagent-free flow-injection amperometric sensor for quantification and speciation of iron for bio-hydrometallurgical applications, Sensors Actuators B. 220 (2015) 448–455.
[43] A. Ghahremaninezhad, D.G. Dixon, E. Asselin, Kinetics of the ferric–ferrous couple on anodically passivated chalcopyrite ($CuFeS_2$) electrodes, Hydrometallurgy. 125–126 (2012) 42–49.
[44] R. Yu, J. Tan, P. Yang, J. Sun, X. Ouyang, Y. Dai, EPS-contact-leaching mechanism of chalcopyrite concentrates by *A. ferrooxidans*, Trans. Nonferrous Met. Soc. China. 18 (2008) 1427–1432.
[45] M.M. Antonijevic, R.P. Mihajlovic, B.V. Vukanovi, Natural monocrystalline pyrite as sensor for potentiometric redox titrations. Part I. titrations with permanganate, Sensors 2 (2002) 153-163.

[46] M. Vuković, B. Pesic, N. Štrbac, I. Mihajlović, M. Sokić, Linear polarization study of the corrosion of iron in the presence of *Thiobacillus ferrooxidans* bacteria, Int. J. Electrochem. Sci. 7 (2012) 2487–2503.

[47] R.M. Luna-Sánchez, I. González, G.T. Lapidus, Limitations for the use of Evans' diagrams to describe hydrometallurgical redox phenomena, in: Electrometall. Environ. Hydrometall., John Wiley & Sons, Inc., Hoboken, NJ, USA, 2013: pp. 1141–1150.

[48] A. Saavedra, V. Garcia-Meza, E. Cortón, I. González, Understanding galvanic interactions between chalcopyrite and magnetite in acid medium to improve copper (Bio)Leaching, Electrochim. Acta. 265 (2018) 569-576.

[49] D. de la Fuente, I. Díaz, J. Simancas, B. Chico, M. Morcillo, Long-term atmospheric corrosion of mild steel, Corros. Sci. 53 (2011) 604–617.

[50] Z. Shi, M. Liu, A. Atrens, Measurement of the corrosion rate of magnesium alloys using Tafel extrapolation, Corros. Sci. 52 (2010) 579–588.

[51] G. Gu, X. Sun, K. Hu, J. Li, G. Qiu, Electrochemical oxidation behavior of pyrite bioleaching by *Acidthiobacillus ferrooxidans*, Trans. Nonferrous Met. Soc. China. 22 (2012) 1250–1254.

[52] B.C. Worley, W.A. Ricks, M.P. Prendergast, B.W. Gregory, R. Collins, J.J. Cassimus, R.G. Thompson, Anodic passivation of tin by alkanethiol self-assembled monolayers examined by cyclic voltammetry and coulometry, Langmuir. 29 (2013) 12969–12981.

[53] S. Carbajosa, M. Malki, R. Caillard, M.F. Lopez, F.J. Palomares, J.A. Martín-Gago, N. Rodríguez, R. Amils, V.M. Fernández, A.L. De Lacey, Electrochemical growth of *Acidithiobacillus ferrooxidans* on a graphite electrode for obtaining a biocathode for direct electrocatalytic reduction of oxygen, Biosens. Bioelectron. 26 (2010) 877–880.

[54] A.G. Lappin, C.A. Lewis, W.J. Ingledew, Kinetics and mechanisms of reduction of rusticyanin, a blue copper protein from *Thiobacillus ferrooxidans*, by inorganic cations, Inorg. Chem. 24 (1985) 1446–1450.

[55] G. Malarte, G. Leroy, E. Lojou, C. Abergel, M. Bruschi, M.T. Giudici-Orticoni, Insight into molecular stability and physiological properties of the diheme cytochrome CYC 41 from the acidophilic bacterium *Acidithiobacillus ferrooxidans*, Biochemistry. 44 (2005) 6471–6481. doi:10.1021/bi048425b.

[56] L. Keller, L.E. Murr, Acid-bacterial and ferric sulfate leaching of pyrite single crystals, Biotechnol. Bioeng. 24 (1982) 83–96.

[57] Y. Liu, Z. Dang, P. Wu, J. Lu, X. Shu, L. Zheng, Influence of ferric iron on the electrochemical behavior of pyrite, Ionics (Kiel). 17 (2011) 169–176.

[58] W. Liu, X. Zhang, Experimental study of microbial pyrite oxidation: a suggestion for geologically useful biosignatures, Geomicrobiol. J. 32 (2015) 466–471.

[59] J.A. Rojas-Chapana, H. Tributsch, Interfacial activity and leaching patterns of *Leptospirillum ferrooxidans* on pyrite, FEMS Microbiol. Ecol. 47 (2004) 19–29.

Table Caption

Table 1. Corrosion parameters of pyrite for 0K and 0.5K medium, obtained from polarization curves at the beginning and the end of the experiments for: *A. ferrooxidans* culture, sterilized culture and culture medium.

Figure Captions

Figure 1. Detail of the pyrite electrodes used for this study (A) and schematic representation of their configuration (B).

Figure 2. Percentage of attachment of *A. ferrooxidans* on pyrite for 0K and 0.5K medium. The number of cells corresponding to the percentage is also indicated as cells mL^{-1}.

Figure 3. Potentiodynamic polarization curves applying LSV (υ=0.4 mV s^{-1}) for experiments performed in 0K (black) and 0.5K (gray) medium. Solid and dashed lines correspond to the measurements at the beginning and end of the experiment respectively. *A. ferrooxidans* culture (A), sterilized culture (B) y culture medium (C) are shown in the plots. One single replicate is shown.

Figure 4. j_{corr} rate mean values for experiments performed in 0K (white) and 0.5K (black) for *A. ferrooxidans* culture, sterilized culture and culture medium. The error bars represent the standard deviation. The insert shows the j_{corr} rate mean values corresponding to AIC (vertical lines) and MIC (horizontal lines).

Figure 5. Behavior of the corrosion rate obtained from Faraday´s equation for experiments performed in 0K (A, B, C) and 0.5K (D, E, F) medium. *A. ferrooxidans*culture (A, D), sterilized culture (B, E), and culture medium (C, F). Different replicates are shown.

Figure 6.CVs for 0K and 0.5K medium experiments.*A. ferrooxidans* culture (A, D), sterilized culture (B, E) and culture medium (C, F) are shown at the beginning (gray line) and the end of experiments (black line). Current peaks are indicated (a,b,c,d). One single replicate is shown.

Figure 7.SEM images of the pyrite surfaces for experiments performed in 0.5K medium for control (A), *A. ferrooxidans* culture (B), sterilized culture (C) and culture medium (D). The arrows show the etch pits produced by the bacteria. Scale bar 5 µm.

Figure 8. Scheme of MIC process induced by *A. ferrooxidans* showing a mechanism by contact generating the etch pits showed in the SEM image (arrows) obtained for *A. ferroxidans* cultures. Scale bar 2 µm.

Vitae

Albert Saavedra obtained his degree in Microbiology at the University Jorge Basadre Grohmann (Tacna, Peru), and then he finished MSc studies in the Pontifical Catholic University of Valparaíso (Valparaíso, Chile). He was awarded with a CONICET doctoral scholarship, at the LABB (Laboratory of Biosensors and Bioanalysis), at the Department of Biochemistry (School of Sciences, University of Buenos Aires, and IQUIBICEN-CONICET, Buenos Aires, Argentina), supervised by Eduardo Cortón and Edgardo Donati. His main interests are the development of analytical systems for biohydrometallurgy, industrial applications and corrosion study.

Federico Figueredo obtained his degree in Biology at the University of Buenos Aires (Buenos Aires, Argentina). He was awarded with a CONICET doctoral scholarship, at the LABB (Laboratory of Biosensors and Bioanalysis), at the Department of Biochemistry (School of Sciences, University of Buenos Aires, and IQUIBICEN-CONICET, Buenos Aires, Argentina), supervised by Eduardo Cortón. His main interests are the development of analytical devices as sensors, and biosensors for environmental and clinical applications.

Eduardo Cortón, PhD, is Head of the Bioanalysis and Biosensors Laboratory in the Biochemistry Department at the Faculty of Science and Maths, University of Buenos Aires, Argentina. He is also an active Independent Researcher at the National Council of Scientific and Technical Research (CONICET). He has published over 70 peer-reviewed research articles and proceedings at international conferences. He is the co-author of the First and Second Edition of *Bioanalytical Chemistry*, and several other books and book chapters. Main research interests are related to biosensor development, microbial fuel cell studies, as well as other related bioelectrochemical systems.

Ximena C. Abrevaya, PhD, is Senior Research Scientist at thethe National Council of Scientific and Technical Research (CONICET), currently working at Instituto de Astronomía y FísicadelEspacio, University of Buenos Aires-CONICET. She is the head of the Argentinian Research Unit in Astrobiology. She obtained her PhD in Biological Sciences at the Universiy of Buenos Aires, Argentina. She has been working in the astrobiology field for more than 10 years, developing novelty biolectrochemical methods for the *in-situ* detection of life in other planetary bodies, among other research topics. Her main research interests are related to planetary habitability and life detection.

Table 1. Corrosion parameters of pyrite for 0K and 0.5K medium, obtained from polarization curves at the beginning and the end of the experiments for: *A. ferrooxidans* culture, sterilized culture and culture medium.

Media	t (d)	*A. ferrooxidans* culture			Sterilized culture			Culture medium		
		E_{corr} (mV)	j_{corr} (µA)	R_p (Ω)	E_{corr} (mV)	j_{corr} (µA)	R_p (Ω)	E_{corr} (mV)	j_{corr} (µA)	R_p (Ω)
0K	0	30.1 ± 0.02	0.6 ± 0.1	330.6 ± 98.1	27.01 ± 0.01	0.7 ± 0.1	158.4 ± 36.3	26.1 ± 0.02	1.01 ± 0.1	219.4 ± 98.1
	42	65.4 ± 31.2	6.0 ± 2.1	41.8 ± 11.2	44.2 ± 21.1	0.9 ± 0.04	224.1 ± 51.0	44.1 ± 32.1	1.1 ± 0.01	216.1 ± 74.3
0.5K	0	100.4 ± 43.0	0.64 ± 0.1	197.6 ± 51.2	112.2 ± 44.2	3.3 ± 0.1	462.8 ± 96.2	121.2 ± 53.1	0.9 ± 0.1	145.5 ± 31.1
	12	420.7 ± 70.2	24.5 ± 4.7	7.2 ± 4.3	219.3 ± 100.1	4.6 ± 2.2	400.9 ± 101.2	251.2 ± 100.1	4.6 ± 2.1	60.1 ± 21.1

Highlights

-Approach aimed to distinguish microbiologically from abiotically-induced corrosion.

-Several electrochemical corrosion parameters can be used

-Allows to detect chemolitotrophic metabolism

-Applications in biomining and for *in- situ* life detection

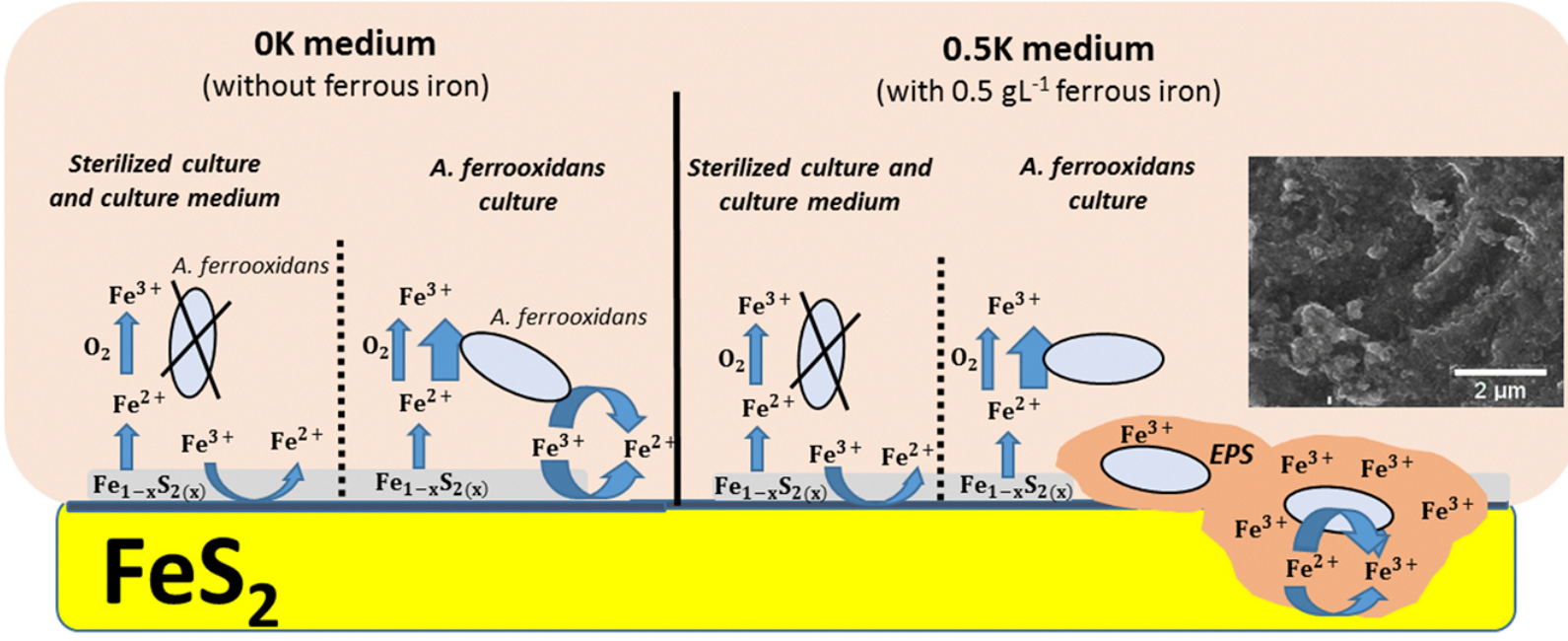

Graphics Abstract

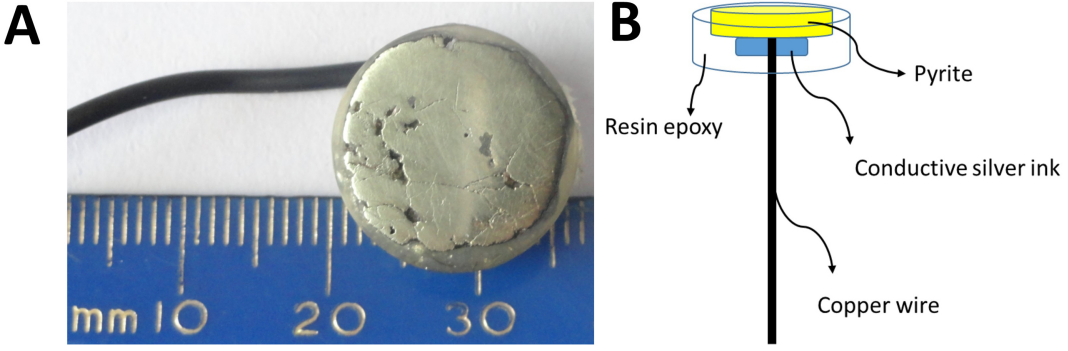
A
mm 10
20
30
B
Pyrite
Resin epoxy
Conductive silver ink
Copper wire

Figure 1

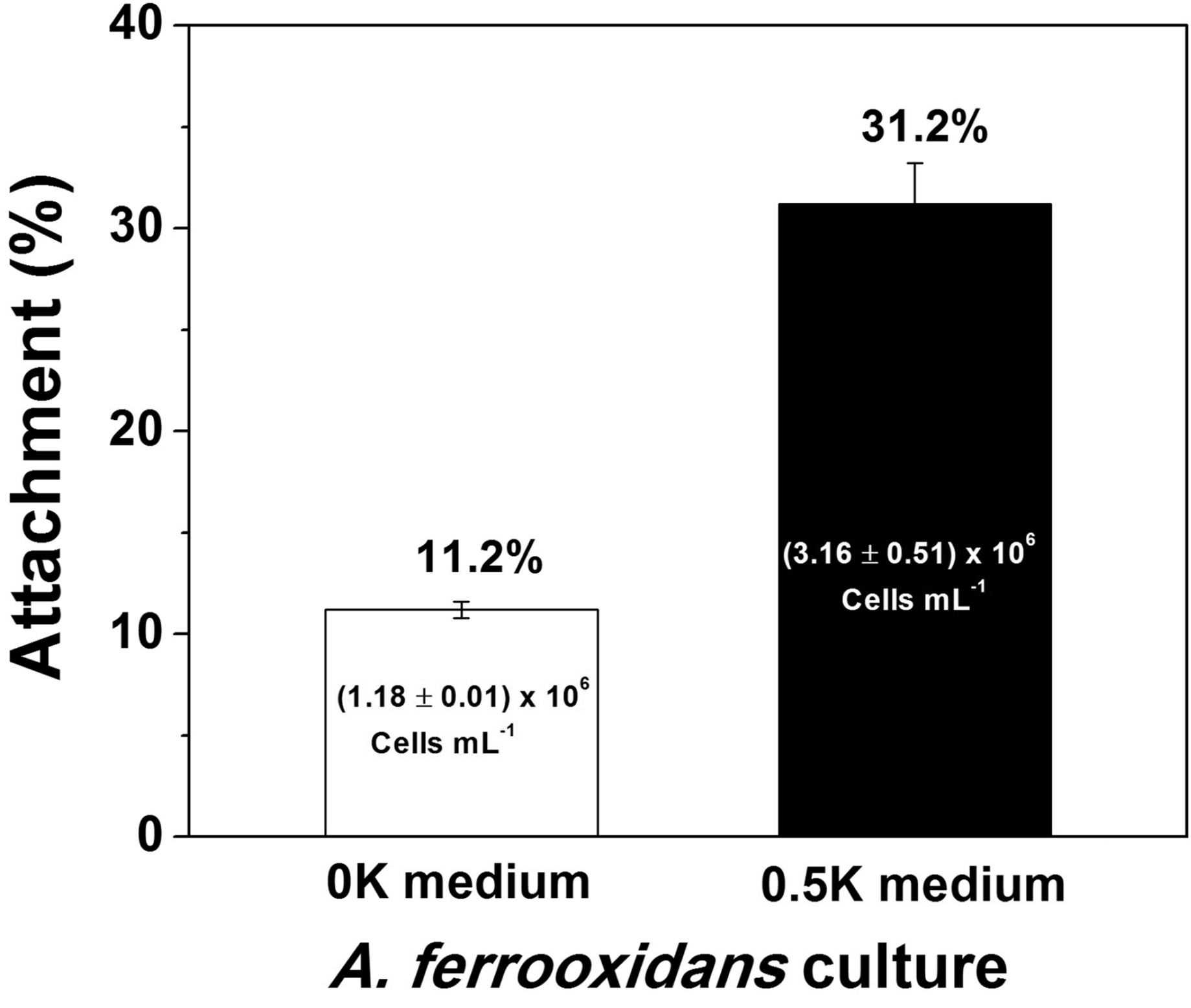
40
30
20
10
0
Attachment (%)
31.2%
11.2%
(3.16 ± 0.51) x 10^6
Cells mL^-1
(1.18 ± 0.01) x 10^6
Cells mL^-1
0K medium
0.5K medium
A. ferrooxidans culture

Figure 2

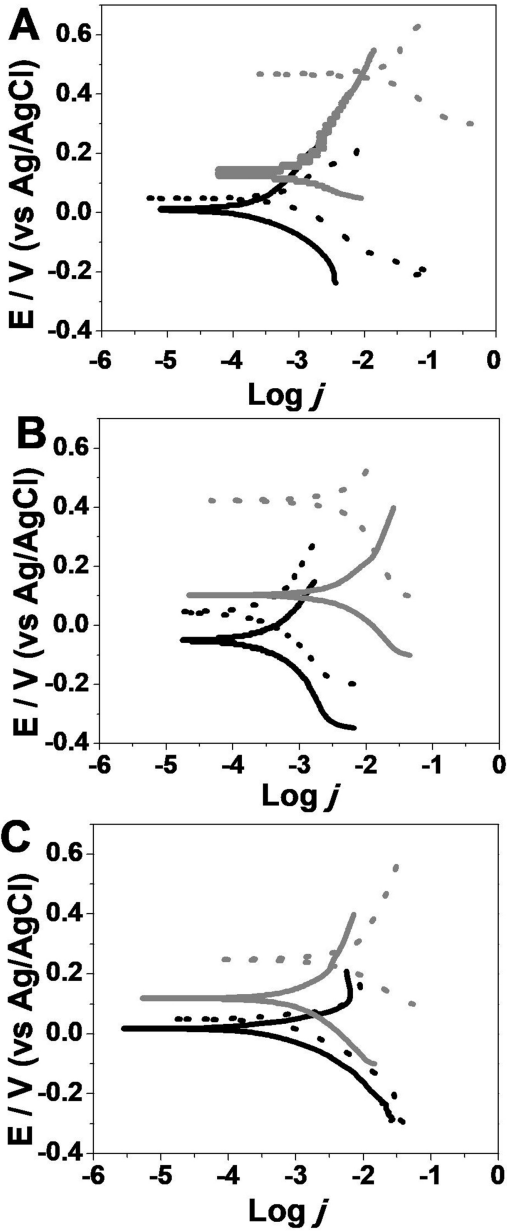

Figure 3

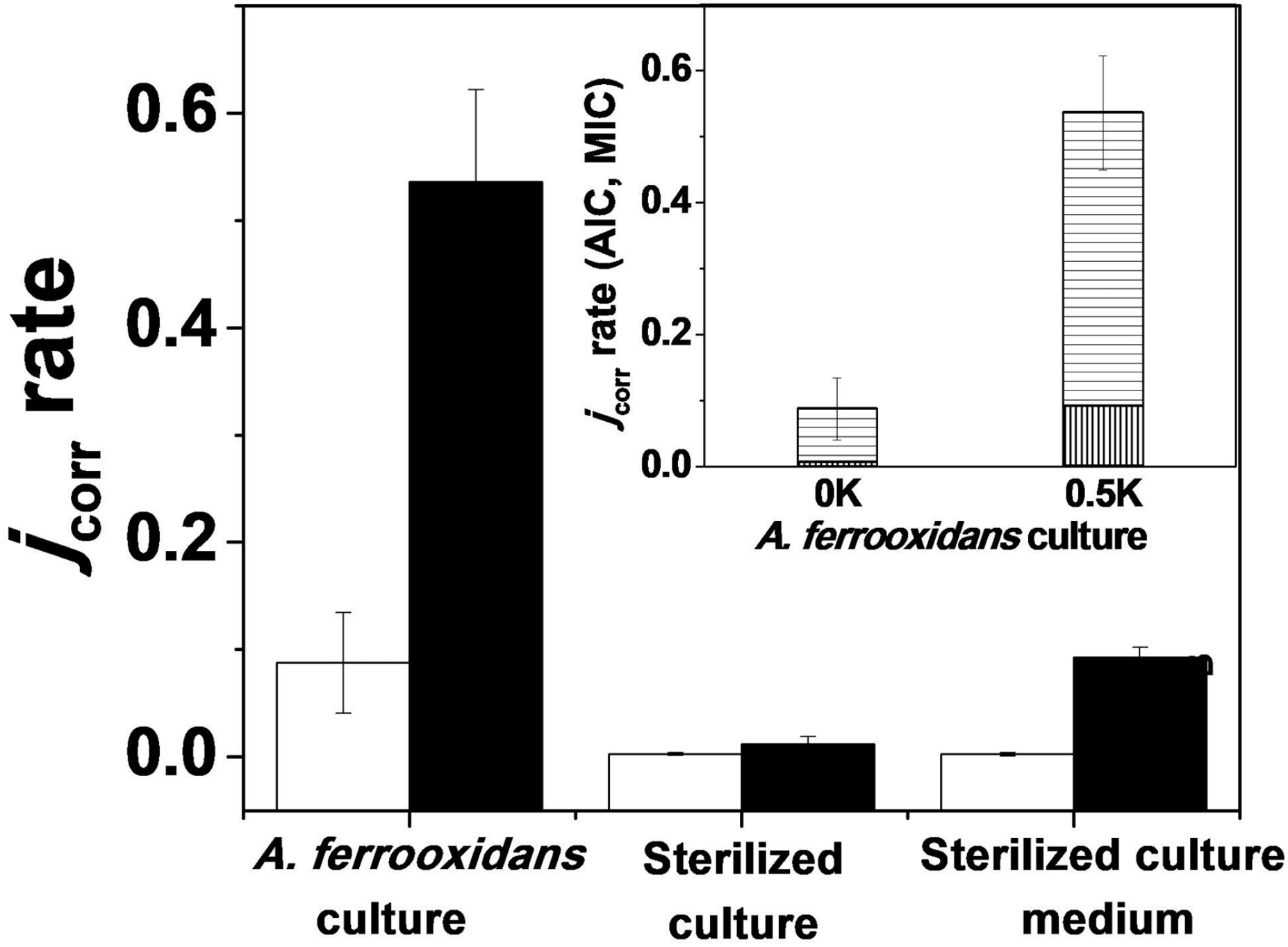
j_{corr} rate
0.6
0.4
0.2
0.0
A. ferrooxidans culture
Sterilized culture
Sterilized culture medium
j_{corr} rate (AIC, MIC)
0.6
0.4
0.2
0.0
0K
0.5K
A. ferrooxidans culture

Figure 4

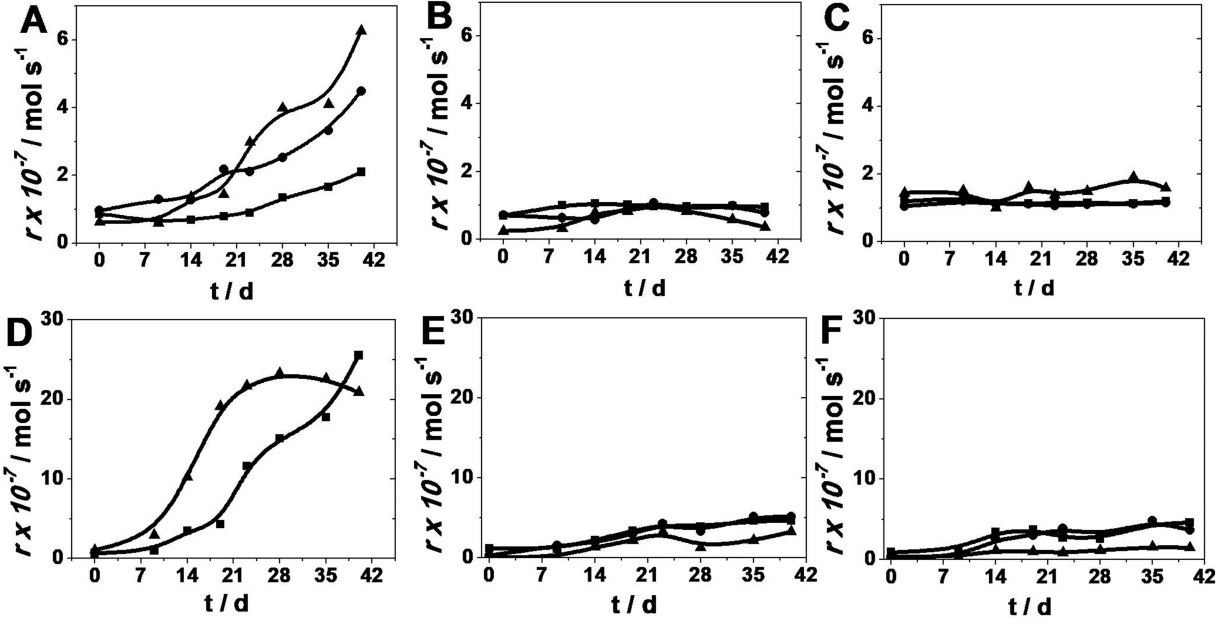

Figure 5

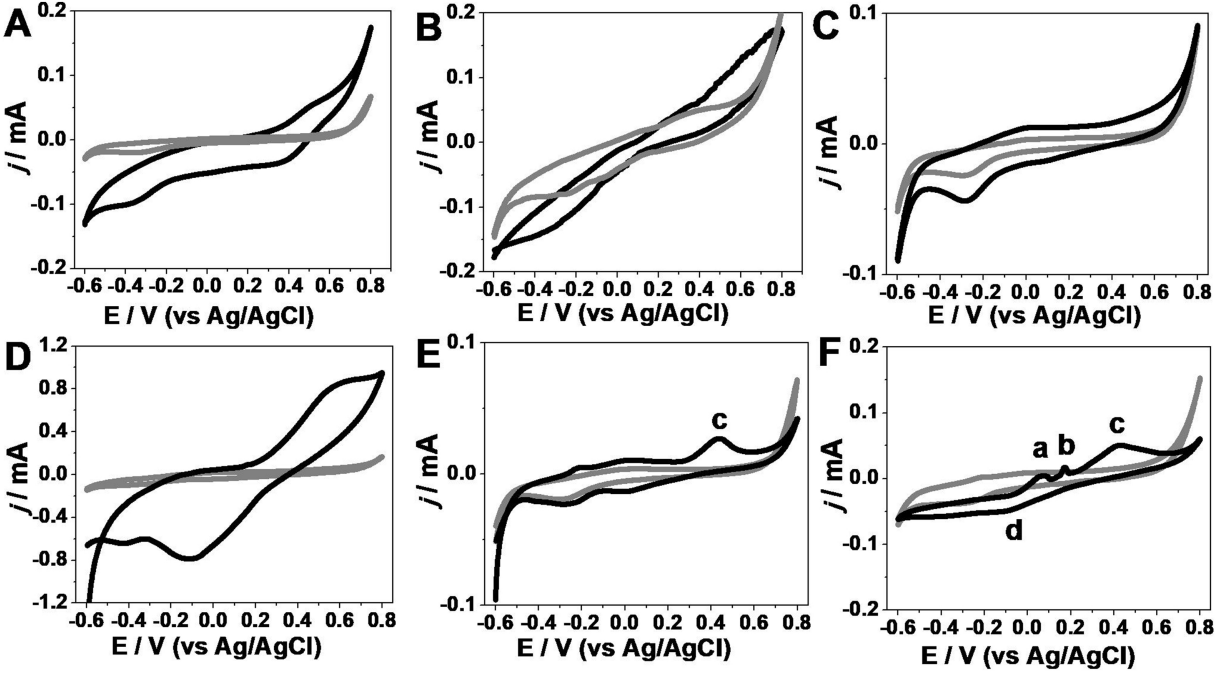

Figure 6

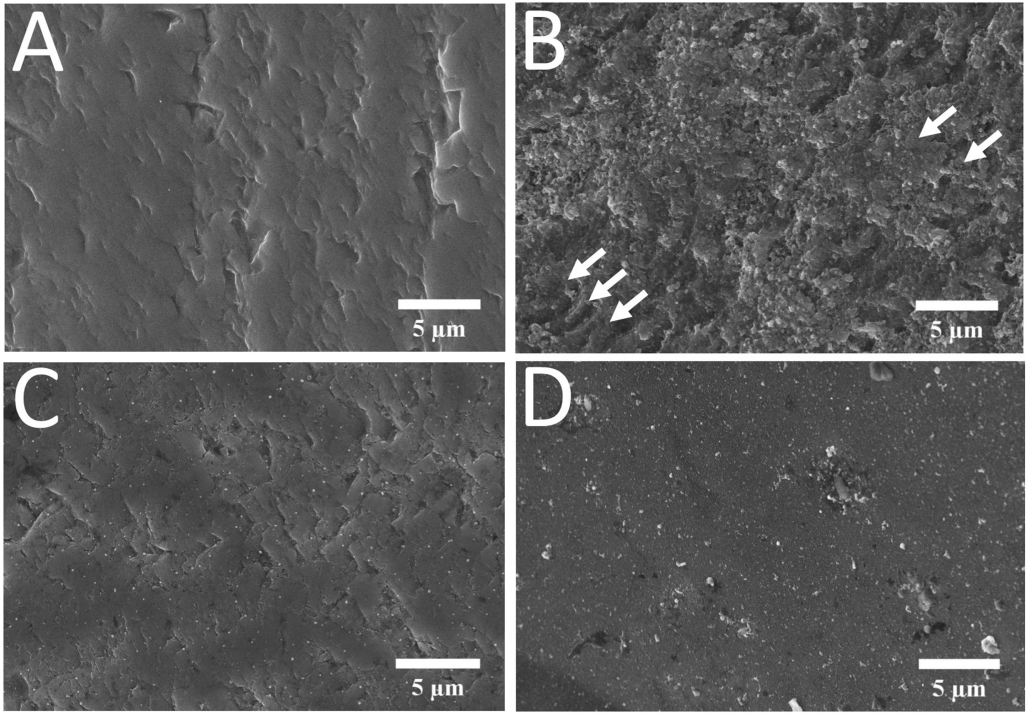

Figure 7

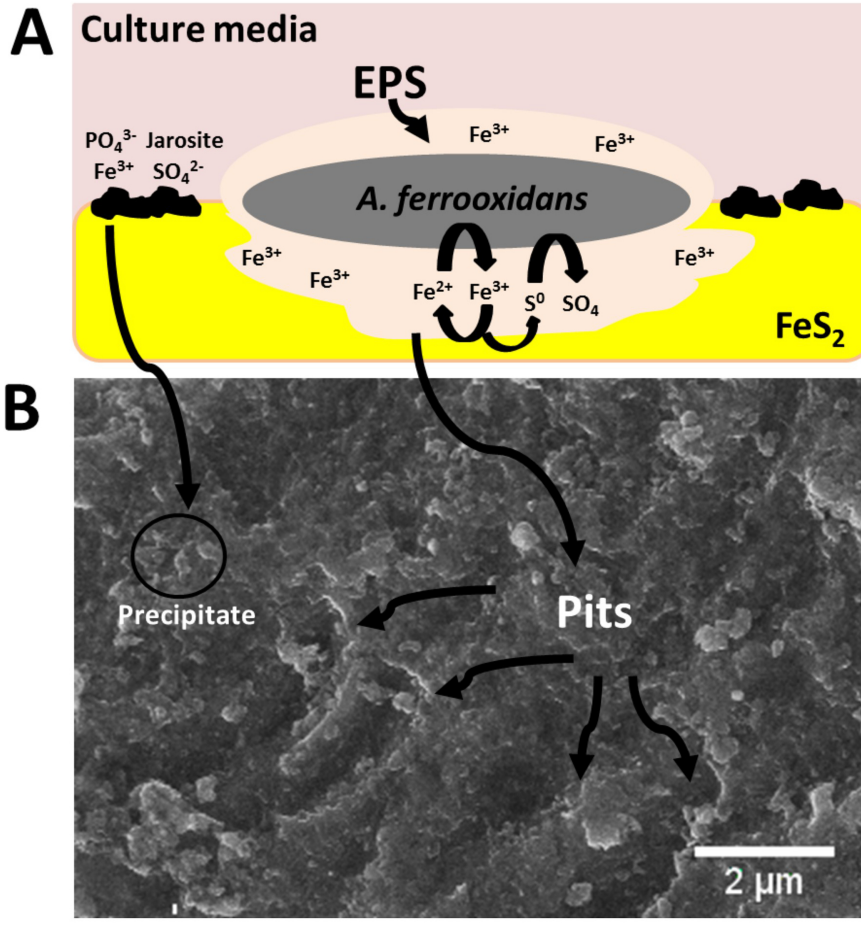
A
Culture media
EPS
PO_4^{3-} Jarosite
Fe^{3+} SO_4^{2-}
Fe^{3+}
Fe^{3+}
A. ferrooxidans
Fe^{3+}
Fe^{3+}
Fe^{3+}
Fe^{2+} Fe^{3+} S^0 SO_4
FeS_2
B
Precipitate
Pits
2 µm

Figure 8